Carbon delivery to deep mineral horizons in Hawaiian rain forest soils

Erika Marin-Spiotta,[1] Oliver A. Chadwick,[2] Marc Kramer,[3] and Mariah S. Carbone[2]

Received 20 October 2010; revised 30 March 2011; accepted 25 April 2011; published 28 July 2011.

[1] This study aimed to better understand the mechanisms for soil organic matter delivery to and accumulation in mineral horizons of tropical rain forest, volcanic soils. We used soil morphology, lysimetry, isotopes, and spectroscopy to investigate the role of preferential flow paths in the delivery of carbon (C) to the subsoil. High rainfall, high primary productivity, and the dominance of highly reactive, short-range-order minerals combine to sequester substantial stocks of soil C with long mean residence times. The soils have large peds, separated by wide cracks, which form a network of channels propagating downward through the top 40 to 60 cm, facilitating macropore flow. The channel infillings and crack surfaces were enriched in organic material (OM) with lower C:N ratios, and had higher ammonium oxalate-extractable Al, and lower ammonium oxalate-extractable Fe than the adjacent mineral bulk soil. CP MAS ^{13}C-NMR spectra of OM accumulating at depth showed strong signal intensities in the carboxyl and carbonyl C regions, indicative of organic acids, while decaying roots showed greater contributions of aromatic and O-alkyl C. The ratios of alkyl-to-O-alkyl C in the organic infillings were more similar to those of the bulk Bh and to dissolved organic matter than to those of decaying roots. Radiocarbon-based ages of OM infillings at >50 cm depth were significantly younger than the mineral soil (2000 years versus 7000 years). Respired CO_2 from incubated soils showed that OM accumulating at depth is a mixture of modern and much older C, providing further evidence for the downward movement of fresh C.

Citation: Marin-Spiotta, E., O. A. Chadwick, M. Kramer, and M. S. Carbone (2011), Carbon delivery to deep mineral horizons in Hawaiian rain forest soils, *J. Geophys. Res.*, *116*, G03011, doi:10.1029/2010JG001587.

1. Introduction

[2] Most soil carbon is stored in mineral-associated forms at depths below 30 cm, although the bulk of our understanding of soil C dynamics still comes from surface horizons [*Nepstad et al.*, 1994; *Richter and Markewitz*, 1995; *Batjes and Sombroek*, 1997; *Jobbágy and Jackson*, 2000; *Lorenz and Lal*, 2005; *Baker et al.*, 2007; *Richter and Mobley*, 2009]. Deep soils have great potential for long-term C stabilization, expressed in C pools with residence times on the order of 1000s of years [*Torn et al.*, 1997; *Trumbore*, 2000, 2009; *Baisden et al.*, 2002; *Rumpel et al.*, 2004]. Understanding the sources and stabilizing mechanisms contributing to the accumulation of soil C at depth is important for predicting the response of deep soil C pools to climatic and other disturbances [*Veldkamp et al.*, 2003; *Trumbore*, 2009]. Dissolved organic matter (DOM) plays an important role in deep soil C storage, by moving fresh organic matter away from surface zones of high microbial activity to deeper horizons [*Michalzik et al.*, 2003; *Schwendenmann and Veldkamp*, 2005; *Schrumpf et al.*, 2006; *Fontaine et al.*, 2007; *Kalbitz and Kaiser*, 2008].

[3] Across a volcanic soil development gradient in the Hawaiian archipelago, greatest soil C storage was measured in deep mineral horizons in an intermediate weathering stage where the soils were rich in metastable short-range-order (SRO) minerals, such as ferrihydrite and allophane [*Torn et al.*, 1997; *Chorover et al.*, 2004]. Soil C stocks and ^{14}C based mean residence times were strongly and positively correlated with concentrations of ammonium oxalate-extractable Fe, Al and Si, providing clear evidence for mineral control on soil C storage [*Torn et al.*, 1997]. The present research addresses potential mechanisms for C accumulation at depth, specifically the delivery of dissolved and particulate organic matter (OM) via preferential pathways generated by the shrinking and swelling of SRO minerals to a very stable, deep soil C pool. The importance of preferential flow paths in the vertical transport of reactive solutes has received recent attention [*Ellerbrock et al.*, 2009; *Leue et al.*, 2010], but their role in the movement and storage of soil C is still unknown [*Chabbi et al.*, 2009].

[1]Department of Geography, University of Wisconsin-Madison, Madison, Wisconsin, USA.
[2]Department of Geography, University of California, Santa Barbara, California, USA.
[3]Earth and Planetary Sciences Department, University of California, Santa Cruz, California, USA.

0148-0227/11/2010JG001587

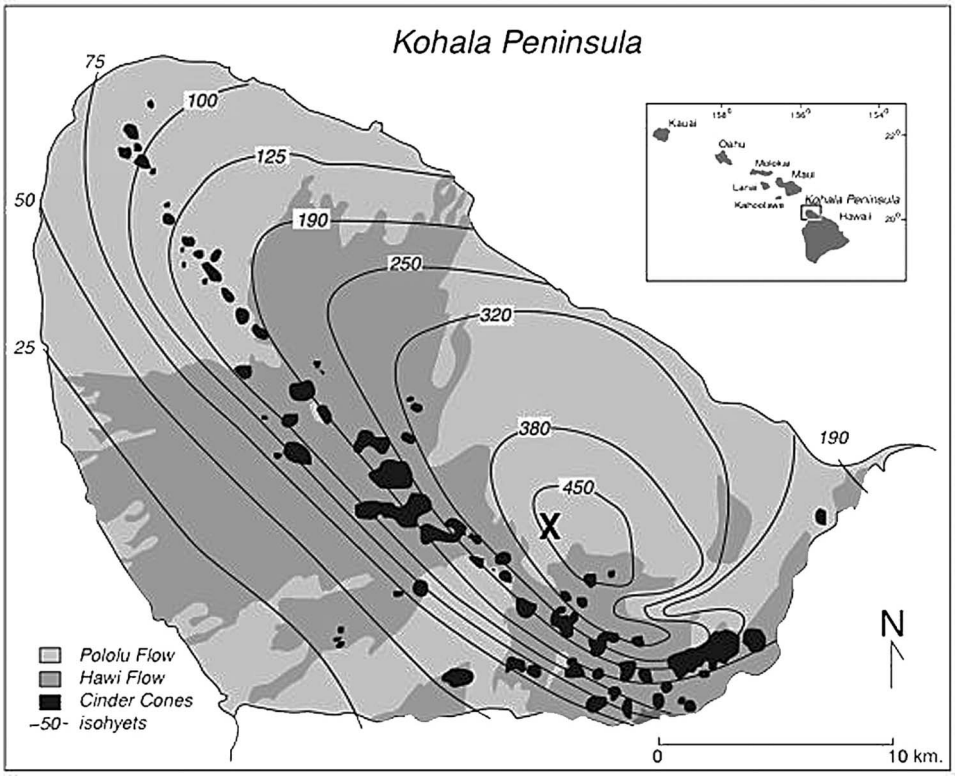

Figure 1. Map of the Kohala peninsula, Hawai'i, showing location of the Pu'u Eke study site, marked by an X, on the Pololu flow. Rainfall isohyets are in units of centimeters.

[4] Andisols contain large amounts of reactive SRO minerals that can easily sorb C compounds and should exhibit little or no translocation of DOM and metals [*Ugolini et al.*, 1988; *Ugolini and Dahlgren*, 2002]. However, SRO-rich soils in Hawaii show evidence of significant transport of C, Al, and Fe down the soil profile. We combined field observation with a variety of analytical techniques to determine the source of C accumulating in B horizons within a volcanic soil dominated by allophane under native tropical rain forest. We measured concentrations of DOM and metals from soil lysimeters and characterized C content, radiocarbon ages, stable C and N isotopic composition, and soil organic matter (SOM) chemistry using solid-state cross polarization magic angle spinning (CP MAS) ^{13}C-nuclear magnetic resonance (NMR) spectroscopy, throughout sequentially deeper organic and mineral horizons. In addition, we performed a short-term laboratory incubation to identify the source of microbially respired C in deep soil horizons. In this highly productive rain forest, we propose that a major source of C at depth is OM produced in the organic horizons and transported through preferential pathways down the soil profile in both dissolved and particulate form to deeper mineral horizons, where it becomes stabilized by sorption onto SRO minerals.

2. Methods

2.1. Site Description

[5] The research was conducted in a rain forest dominated by O'hia (*Metrosideros polymorpha* (Myrtaceae)) and the tree fern Hapu'u pulu (*Cibotium splendens*) that is supported by soil formed on a ca. 350 ka Pololu pahoehoe flow [*Chadwick et al.*, 2003; *Wolfe and Morris*, 1996; *Spengler and Garcia*, 1988] on the slopes of Pu'u Eke at 1800 m altitude on Kohala mountain, Hawai'i (20°4′42″N, 155°43′44″W; Figure 1). The soil has udic bordering on perudic moisture regime with mean annual rainfall of about 3000 mm, although due to the lack of measurement stations in the immediate area, estimates of mean annual rainfall may range between about 2800 to 3500 mm [*Giambellucca et al.*, 1986]. Interannual variation in rainfall is high; variability recorded at nearby rainfall stations on Kohala Mountain (e.g., Headquarters Site) suggests year-to-year variation of 25% mean annual precipitation. Based on the atmospheric temperature lapse rate, the site has a mesic temperature regime with mean annual temperature of about 15°C. The sampling area is located on constructional topography with slopes between 2 to 5%. Although the soils exhibit little evidence of substantial long-term erosion, there is evidence for surface horizon erosion and disturbance caused by feral pigs introduced to the island by Polynesians and Europeans. Soils on the constructional Pololu flows have long residence times [*Porder et al.*, 2007; *Porder and Chadwick*, 2009] and hence have been influenced by variation in long-term climate. The most significant component of this is a period of drying of 5–10 thousand year duration during the last full glacial period (and likely during previous full glacial periods) when the top of Kohala Mountain was above the tropical rainfall inversion layer [*Hotchkiss et al.*, 2000; *Chadwick et al.*, 2003]. Based on chemical and mineralogical analysis of soils along climate gradients on Kohala Mountain and along chronosequences across the Hawaiian Islands, we believe that the dominant soil properties reflect the longer

Table 1. Selected Pedological Properties for a Representative Soil Profile at Pu'u Eke[a]

Soil Horizon	Depth (cm)	Bulk Density (g/cm^3)	pH	CEC (mEq/100 g soil)	Al-p (%)	Al-o (%)	Al-d (%)	Fe-p (%)	Fe-o (%)	Fe-d (%)	Si-o (%)	C (%)	N (%)
Oie	0–2											43.6	1.0
Oa	2–10	0.19										35.4	1.9
Oa/Bh	10–12		3.7	64.3	0.1	0.1	0.2	0.6	0.9	0.8	0.1	36.8	2.0
Bh1	12–20	0.28	4.2	118.3	1.6	1.3	1.7	5.1	9.9	6.8	0.2	20.9	1.1
Bh-organic matter	20		4.2	133.0		2.3			7.2			29.7	1.3
Bh2	20–28	0.30	4.0	106.1	1.8	1.7	1.8	6.5	12.3	8.4	0.2	22.3	1.2
Bhsg	28–39	0.36	4.2	79.9	2.2	2.3	2.0	2.0	3.4	2.1	0.2	20.3	0.9
Bhsm	38–43	0.69	4.7	72.6	2.4	4.1	3.9	7.5	14.4	10.2	0.5	10.3	0.2
Bg1	43–58	0.49	4.2	60.3	2.4	11.7	5.3	2.1	3.8	2.3	3.0	8.1	0.2
Bs	58–79	0.46	4.4	114.5	4.9	14.7	8.5	6.8	16.2	8.1	3.0	8.8	0.2
Bsh-organic matter	66		4.7	108.8		10.7			1.6			20.9	0.9
Bsm	79–86	0.66	4.6	64.2	2.3	10.7	4.7	3.2	13.1	7.4	2.5	8.3	0.2
Bg2	86–110	0.52	4.5	96.3	2.7	14.0	5.0	2.2	2.6	2.9	3.9	5.3	0.1
Cr	110–125+		4.5	79.3	0.7	11.3	1.5	0.1	1.0	1.6	4.3	5.0	0.1

[a]See section 2 for more details on analyses and extraction procedures. CEC = cation exchange capacity; Al-p and Fe-p = pyrophosphate extractable; Al-o, Fe-o, and Si-o = acid ammonium oxalate extractable; Al-d and Fe-d = dithionite citrate extractable. Organic matter samples at Bh and Bsh represent organic accumulations along ped surfaces and in macropore channels.

periods of wet conditions, particularly during the last 10 thousand years [*Chadwick et al.*, 2003]. The soil profiles at our study site classify as medial, ferrihydritic, isomesic, acrudoxic Hydric Hapludands or medial ferrihydritic isomesic Hydric Placudands. The primary difference between these two classes is that some profiles have thin (1–5 cm) placic layers, which are Fe, Mn and organic matter cemented laminae that form along flow paths in subsurface horizons [*Soil Survey Staff*, 1999]. Characteristic soil properties are shown in Table 1.

[6] We identified a 25 m × 25 m area that had uniform slope and minimal surface disturbance where we could insert rainfall and throughfall collectors as well as zero tension and tension lysimeters within soil horizons without encountering much spatial variation. It was in fact this spatially distributed approach that led to our recognition of the importance of the soil cracks that form the basis of this paper. Hence, not withstanding the slight difference in soil classification, we treat the individual profiles that are reported in this paper as being representative of the variation within a single soil body on the landscape, a polypedon [*Soil Survey Staff*, 1999].

[7] Detailed horizon-based descriptions of soil morphology were conducted on three soil pits dug to weathered bedrock or to 1 m depth, whichever came first. We selected locations for pits where surface soil was minimally disturbed by feral pig activities. Each horizon was channel sampled, supplemented by nonbulked samples from transition zones separating A and B horizons, oxidized and reduced layers, and in locations where we identified placic laminations. Bulk density was measured on intact clods that were coated with saran in the field and then recoated in the laboratory [*Blake and Hartge*, 1986]. Samples were also collected from organic matter fillings in channels and coatings on peds surfaces (described below). Soils (except those for incubations, see below) were refrigerated and shipped to the University of California, Santa Barbara for analysis.

2.2. Soil Morphology

[8] Undisturbed soils had well-developed (thick) organic horizons (Table 1). The forest floor was covered by an approximately 2 cm thick Oie layer composed primarily of O'hia and fern leaves, with interspersed patches of moss, 3–4 cm thick. Soils contained multiple Oa and Bh horizons and a transitional horizon (Oa/Bh). The thickest Oa horizons were found beneath mossy patches. The Bh horizons were well developed, dark in color, and up to 8 cm thick (Figure 2). Below the Bh, horizons showed redoximorphic features in terms of oxidized/reduced zones, mottles and red coatings on peds, suggesting a fluctuating water table. The soil profile commonly showed discontinuous near horizontal, cemented, or placic, layers near 40 cm, often with a second placic layer at 80 cm. Along with high rainfall, the placic layers are responsible for maintaining poor drainage conditions in the upper portion of the soil, resulting in episaturation and development of gleyed (Bg) horizons immediately above and below the zone of reduced permeability. The deepest horizons tended to be well drained and did not show redoximorphic properties. The downward movement and accumulation of organic matter was extensive, with the presence of humic properties as deep as 60 cm, especially where the placic horizon was not well developed. These appeared as distinct dark pockets of loose organic matter (Figure 2), and sometimes as thickened black horizontal layers at multiple depths.

[9] A common characteristic of these soils was the mixed boundary between the Bh and Bs/Bg horizons, due to illuvial OM, root growth, and physical mixing. Mixing in these soils appeared to be a result of shrinking and swelling of large peds and tree uprooting. Macroinvertebrate activity is very low in Hawaiian forest soils, so that faunal mixing in areas not disturbed by feral pigs was minimal. Areas disturbed by feral pig rooting and wallowing activities showed complete loss of O horizons and weakening of the Bh horizon, if present at all. Disturbed areas had poor drainage as evidenced by standing pools of water after strong rain events.

[10] Soil structure was moderate to strong and large peds were separated by cracks up to 1.5 cm wide (Figure 2), which could facilitate macropore flow. Channel openings, cracks, and loose organic matter pockets were very prevalent at the top of the Bh horizon, where they appeared to originate. These cracks became much more visible after prolonged drying associated with periodic drought, even from one year to the next, suggesting they are developed by shrinkage and swelling of the soil. Cracks propagated downward through

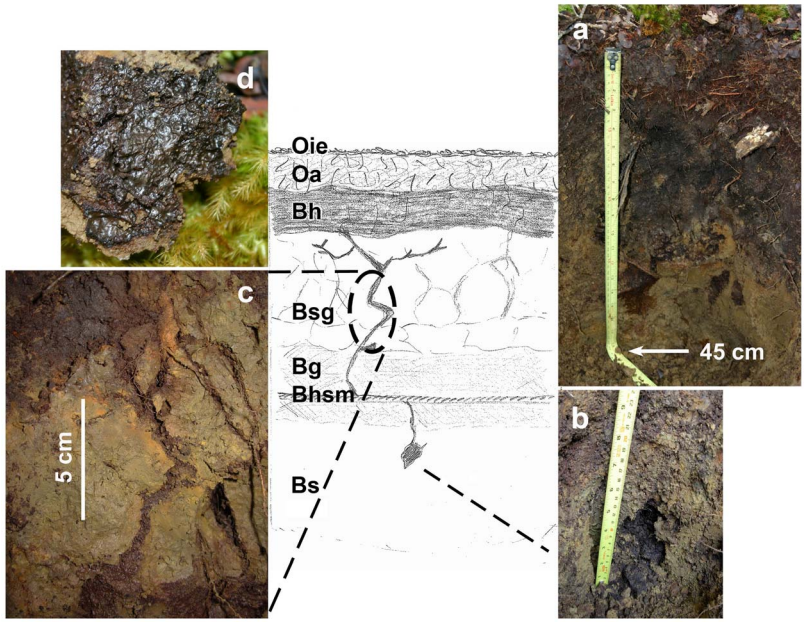

Figure 2. Sketch of representative soil profile showing sequence of horizons in an intermediate weathering age site under tropical rain forest at Pu'u Eke in Hawai'i. Profiles have well-developed Oa and Bh horizons and a single or multiple placic layers (Bhsm) and exhibit the presence of a network of cracks delivering organic matter from surface depths to deeper mineral horizons. Photos highlight organic accumulations and preferential flow paths in the soil profile. (a) Vertical profile of open pit with evidence of the physical translocation of dark brown and black humic material from the Bh down the soil profile, (b) dark organic matter pocket at 50–60 cm depth, (c) enlargement of a system of cracks and channels coated in dark brown organic matter and showing oxidation of Fe along the edges, and (d) enlargement of dark organic coatings on ped surfaces.

the top 40 to 60 cm, terminating at the top of the Bw horizons where they often merged into the near horizontal placic layers (Figure 2). In addition to serving as preferential water flow paths, cracks were the locus for root and fungal growth. Soil bulk densities were low, typical of andic soils (Table 1); they averaged 0.41 ± 0.13 g cm^{-3} toward the surface, peaked at 0.73 ± 0.23 g cm^{-3} in the placic horizons in the 40–60 cm depth range, and decreased to an average of 0.61 ± 0.08 g cm^{-3} at the lowest soil depths.

2.3. Soil Characterization

[11] In the lab, soils were air-dried, passed through a <2 mm mesh sieve, homogenized, and lightly ground using a mortar and pestle. Field moist samples were extracted for Fe, Al, and Si with 0.1 M sodium pyrophosphate, 0.2 M ammonium acid oxalic acid (pH = 3.0), and 0.3 M dithionite citrate following methods adapted from *Soil Survey Laboratory Staff* [1992], *Bascomb* [1968], *McKeague and Day* [1966], *Mehra and Jackson* [1958], and *Wada* [1989]. These fractions are operationally defined and we make the following assumptions. Fe in primary mineral or recalcitrant forms is calculated by subtracting dithionite citrate extractable (Fe-d) from total Fe in the horizon. The oxalate extractable metals (Fe-o, Al-o, Si-o) are believed to be complexed with SRO minerals. Fe in strongly crystalline forms is calculated by subtraction of the oxalate extractable Fe from the dithionite extractable value. Soil extracts were analyzed on an atomic absorption (AA) spectrometer. Soil samples were extracted with 1N NH_4Oac buffered at pH 7 and analyzed on an AA for cations and extracted with 1N KCl and analyzed on a Lachat AE ion analyzer for anions. Soil pH was measured in the supernatant of a 2:1 water to soil solution with bench top meters.

[12] Total soil C and N concentrations and stable isotopes were measured with a coupled continuous-flow elemental analyzer-isotope ratio mass spectrometer (EA-IRMS) system with a Carlo-Erba model 1108 EA interfaced to a Thermo-Finnigan Delta Plus XP IRMS at the light stable isotope facility of the University of California, Santa Cruz. Dry samples (<2 mm) were ground finely with a zirconium mortar and pestle, and loaded into tin boats. Stable isotope data are reported relative to atmospheric air for $\delta^{15}N$. Analytical precision of in-house standards, which had been calibrated using international standards, was typically better than 0.2 per mil for $\delta^{15}N$. Analysis of internal standards indicated an analytical error of <5% for N and <2% for C. C:N ratios are reported based on moles of C and N.

2.4. Microbial Biomass

[13] Microbial biomass C and N were measured following *Fierer and Schimel* [2003]. Three replicate 10 g field moist subsamples from bulk soils collected from the Bh, Bhsg and Bw horizons were extracted in 40 mL of 0.5 M K_2SO_4 with and without $CHCl_3$. Fumigated samples received 0.5 mL of liquid $CHCl_3$. Unfumigated extracts were shaken for 2 h and fumigated extracts for 4 h at 150 rpm and vacuum filtered

through 1 μm Type A/E glass fiber filters (Pall Life Sciences, NY). Fumigated extracts were sparged with air for 20 min to remove $CHCl_3$. All samples were stored at −20°C until further analysis. Total dissolved C and N concentrations were measured on thawed fumigated and unfumigated extracts by persulfate digestion [*Cabrera and Beare*, 1993]. Digests were analyzed colorimetrically by flow injection on a Lachat AE ion analyzer, modified to measure both CO_2 and NO_3^- as described by *Doyle et al.* [2004]. C and N concentrations were corrected for instrument drift, for C and N recovery using glycine and dextrose standards, and with sample blanks (extract and matrix solutions without soil).

2.5. Solution Samples

[14] Water chemistry was measured from approximately 28 overnight rainfall events from May 2007 through July 2008. Rainwater and throughfall were sampled from two to three bucket collectors placed in a gap opening at the edge of the forest and from five to seven funnel collectors placed in the forest to capture the heterogeneity of the canopy, respectively. Water percolating through the Oie horizon was collected from five zero-tension funnel lysimeters attached to Nalgene 1 L bottles. Six zero-tension pan lysimeters were buried under the Oa horizon. The three pits excavated for soil pedon characterization were instrumented with ceramic cup tension suction soil water samplers (Model 1900 Soilmoisture Equipment Corp., Santa Barbara, CA) in the Bh (two replicates), Bg (two replicates), and Bw (one replicate) horizons. The suction soil lysimeters were attached to a glass flask, which collected water when pulled to vacuum with a hand pump. All lysimeters were conditioned in the field for at least 4 months before sampling. Samples were collected after rain events from lysimeters that had been emptied and evacuated (in the case of the tension lysimeters) the night before. Data reported are averages across all sampling dates. Total dissolved Fe and Al were measured on a Perkin-Elmer Optima 4300 DV ICP Optical Emission Spectrometer and total organic C and total N were measured on a Shimadzu TOC-VCPH TC/TN Analyzer at the Marine Analytical Lab at UC Santa Cruz.

2.6. NMR Spectroscopy

[15] Solid-state ^{13}C-NMR spectroscopy provides data on the relative abundance of organic C functional groups, which can be used as indicators for different compound types [*Kögel-Knabner*, 1997, 2000; *Preston*, 2001]. Solid-state VACP MAS ^{13}C-NMR spectra were acquired on a Bruker AVANCE 300 MHz NMR spectrometer in the Materials Research Lab at U.C. Santa Barbara for organic matter collected primarily from thickened, black layers and pocket infillings from two depths: 20 cm and 60 cm, and from decaying root channels. In addition, spectra were generated for the Ag (Bh) bulk horizon (15–25 cm depth) and for bulk O horizon leachate (DOC) (M. G. Kramer, unpublished data). Samples were packed in Bruker 4 mm diameter zirconia rotors with kel-f caps and spun at 10 kH in a 5 mm HXY MAS probe. The optimum cp contact time was 1 ms, the proton 90 was 4.5 μs, and the decoupling field was 55.55 kHz. All spectra were referenced to that of adamantane. Spectra were digitally processed using an exponential weighting equation with a line broadening at 100 Hz and a Fourier transformation on Bruker Topspin NMR software. The software was used to integrate peak areas under the following chemical shift regions (and the general C types they represent): 0–45 (alkyl), 45–65 (methoxyl), 65–95 (O-alkyl), 95–110 (di-O-alkyl and some aromatic C), 110–165 (aromatic) and 165–220 ppm (carboxylic and carbonyl C) [*Baldock et al.*, 2004]. The integrated spectral areas were normalized to the total signal intensity for each spectrum. We used an expanded region for O-alkyl C (45–100 ppm) to calculate ratios of alkyl-C to -O-alkyl-C, which is a commonly used index of decomposition [*Baldock et al.*, 1997].

2.7. Soil Incubations

[16] Laboratory incubations were used to determine the Δ^{14}C of respired CO_2 from the different soil horizons following *Schuur and Trumbore* [2006]. Soils were collected in April 2009 from the Bh, Bhsg, and Bw horizons, and kept at field moisture in coolers with ice packs (but not refrigerated) for less than 4 days until incubations could be set up at UC Santa Barbara. In the lab, each soil sample was homogenized by hand, carefully removing all roots, organic debris, and rocks. Three replicates of approximately 100 g of field moist soils from each horizon were incubated at room temperature in 2 L Mason jars with gas-tight lids. The CO_2 concentration in each jar was measured daily using an IRGA (Licor 6252, Lincoln, NE) to monitor the rate of CO_2 production. After 15 days, enough time for the production rates to stabilize, the jars were flushed with CO_2-free air, and left to accumulate CO_2 for 7–14 days. For ^{14}C analyses, the accumulated CO_2 was collected from the jar head space with an evacuated 0.5 L can.

2.8. Radiocarbon Measurements

[17] The radiocarbon content was determined for bulk-soil horizons, organic coatings and infillings, respired CO_2, and DOC. Soil horizons and organs were oven-dried at 60°C, then homogenized with a mortar and pestle. The DOC was freeze-dried to evaporate all liquid. These samples were then converted to CO_2 by combustion. The CO_2 from these samples, as well as the respired CO_2 collected from the soil incubations were purified on a vacuum line, and converted to graphite using a sealed tube Zn reduction method [*Xu et al.*, 2007]. The ^{14}C content of the graphite was measured using accelerator mass spectrometry (NEC 0.5MV 1.5SDH-2 AMS system) at the W.M. Keck-CCAMS facility of UC Irvine [*Southon et al.*, 2004]. The radiocarbon data (Δ^{14}C) are reported in per mil, and the conventional radiocarbon age (CRA) is used to describe the approximate age of the C [*Stuiver and Polach*, 1977].

3. Results

3.1. Soil C and N Concentrations and Stable Isotopes

[18] Total C and N concentrations decreased exponentially down the soil profile, from 44% C and 1.0% N in the O horizons down to 5% C and 0.1% N in the deeper (Cr) mineral horizons (Table 1 and Figure 3). Soil C:N ratios in the mineral horizons increased with soil depth, from a value close to 20 in the Oa/Bh to between 40 and 55 in the lowest depths, similar to the C:N value of the Oie horizon (Figure 3). The highest mineral soil C:N value was measured in a Bhsm

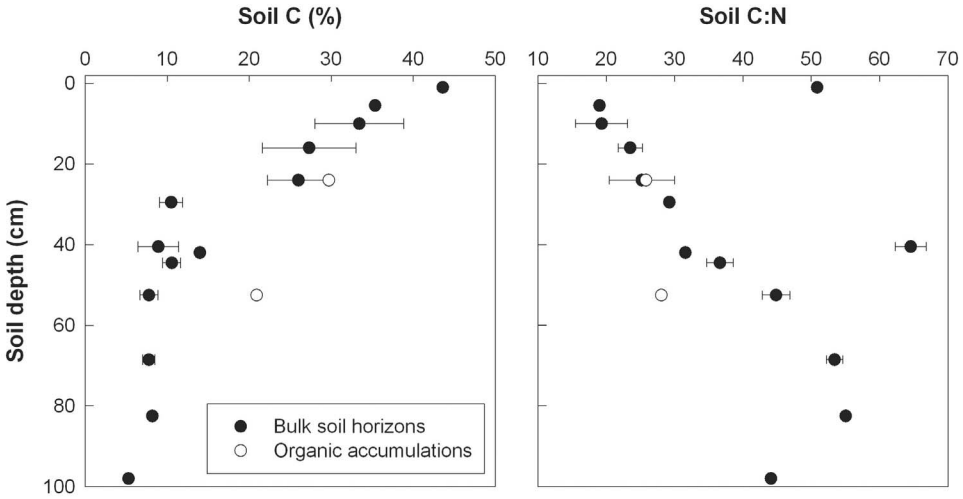

Figure 3. Mean (left) C concentrations (%) and (right) C:N for bulk soil horizons (black circles) and organic coatings on ped surfaces and infillings of macropore channels (open circles) down the soil profile in an intermediate weathering age site under tropical rain forest in Hawai'i.

horizon (43–47 cm), right below a Bg horizon. Soil C concentrations decreased and C:N ratios increased with increasing soil pH (data not shown).

[19] Below the organic horizons, OM visibly accumulated in the mineral soil profile as soft, slimy dark brown and black plugs or layers and as 0.5 to 3 mm thin coatings of waxy coatings along the walls of the cracks (Figure 2). Brown decomposing coarse roots (>2 mm in diameter) were also visible in surface mineral horizons. Organic coatings and macropore infillings had higher oxalate-extractable Al and lower oxalate-extractable Fe compared to the bulk soil in the corresponding mineral horizons (Table 1). The edges of the channels and cracks show visible enrichment of oxidized Fe (Figure 2). Below the Bh, C:N ratios were narrower in the organic infillings than in the bulk soil (Figure 3). Organic matter in decomposing coarse root channels had the widest C:N ratios (43), while most other organic coatings and infillings had C:N ratios in the mid 20s.

[20] Soil C stable isotopes showed typical enrichment in ^{13}C with depth (Figure 4). The Oa horizon was slightly depleted in $\delta^{13}C$ (−30‰) compared to the Oie (−28.8‰). The maximum difference in $\delta^{13}C$ (up to 3.65 ‰) occurred between the Oa1 horizon (2–9 cm depth) and the contact zone between the lowest B and C mineral horizons (76–83 cm depth). Soil $\delta^{15}N$ values showed a different depth pattern (Figure 4). The Oie and Oa1 root samples had $\delta^{15}N$ values of −1.45‰ and −0.27‰, respectively, close to atmospheric values. The Oa2 horizon was enriched in ^{15}N compared to the organic horizons above it, but unlike $\delta^{13}C$, the deeper mineral horizons were significantly depleted in $\delta^{15}N$. The

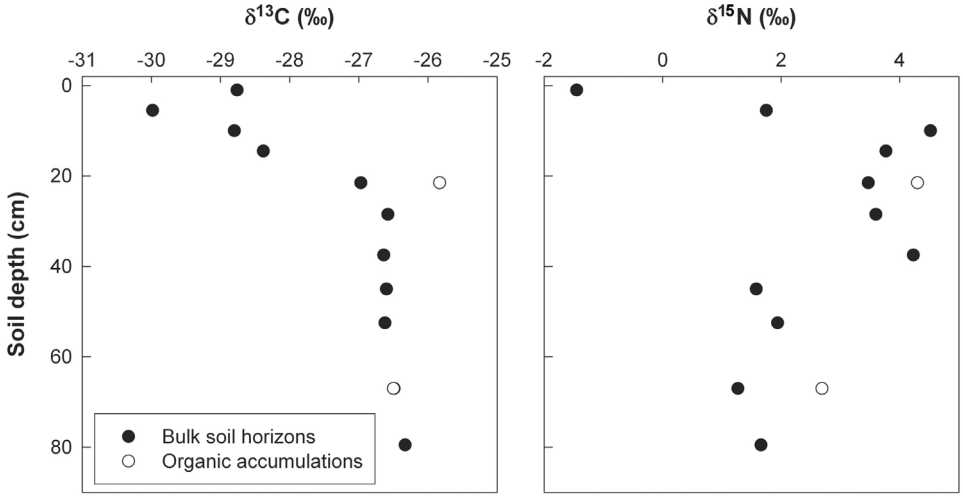

Figure 4. Stable (left) C (‰) and (right) N isotopic composition (‰) for bulk soil horizons (black circles) and organic coatings on ped surfaces and infillings of macropore channels (open circles) down the soil profile in an intermediate weathering age site under tropical rain forest in Hawai'i.

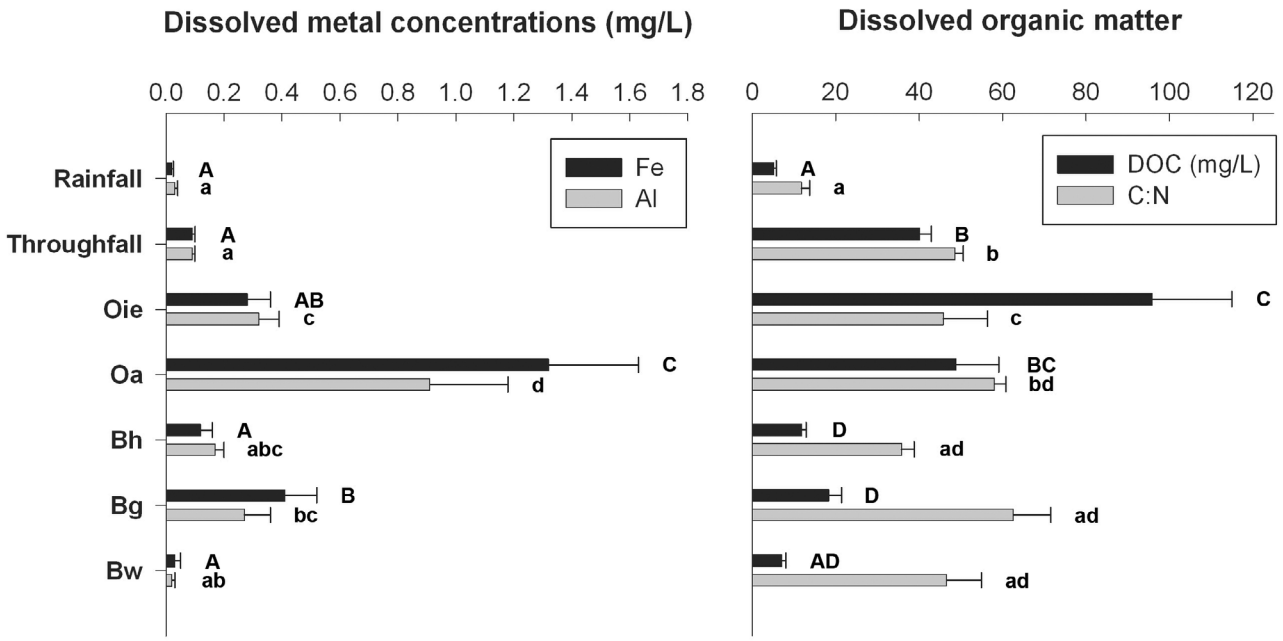

Figure 5. Dissolved (left) Fe and Al concentrations (mg/L) and (right) DOC (mg/L) and C:N ratios in water samples collected from rainfall, throughfall, and lysimeters under the different organic and mineral soil horizons down the soil profile.

^{15}N data showed a clear separation between the horizons above the placic, with high δ^{15}N values and low C:N ratios, and the horizons below the Bhsm, with lower δ^{15}N values, matching that of the Oa1 horizon.

3.2. Dissolved OM, Fe, and Al

[21] DOC concentrations increased under the canopy in throughfall but the greatest production of DOC occurred in the forest floor, in particular in the Oie horizon (Figure 5). Release of dissolved Fe and Al was greatest in the underlying Oa horizon (Figure 5). Solute concentrations decreased significantly in the Bh horizon and DOC remained constant throughout the deeper horizons, averaging between 10 and 20 mg L^{-1}. Total dissolved Fe concentrations increased in the gleyed mineral horizon, most likely due to mobilization of ferrous ions, and decreased in the deeper, more oxidized, Bw horizons. Solution C:N ratios increased below the canopy and remained high (average around 50) throughout the soil profile, even as DOC concentrations varied (Figure 5), matching C:N ratios of deeper soil horizons (Figure 3).

3.3. NMR Spectroscopy

[22] Illuvial organic matter accumulating at depth differed not only morphologically but also chemically from roots decomposing in situ as determined by solid-state ^{13}C-NMR spectroscopy (Table 2 and Figure 6). Decaying coarse roots had stronger signal intensity in the O-alkyl and aromatic C regions and twice the intensity in the phenolic C region as the other types of organic forms. Spectra of decomposing roots were dominated by a peak at 73 ppm, representing carbohydrates, here most likely plant cellulose and hemicellulose. Also important in the decomposing root samples are peaks at 56 and 150 ppm. This aromatic C is probably derived from lignin [*Conte et al.*, 2003], rather than being indicative of black carbon since these forests have not burned recently.

[23] The organic channel infillings and ped coatings measured from thickened accumulations at 20 and 60 cm exhibited strong signal intensities in the alkyl C region, followed by the carboxyl-carbonyl and O-alkyl C regions (Figure 6). The organic infillings had strong signals at 28 ppm, representing

Table 2. Contributions of Different C Functional Groups to Total Spectral Area as Determined by ^{13}C-NMR for Organic Accumulations, Bulk Soil, and DOM at Pu'u Eke

	Alkyl (0–45) (%)	Methoxyl/N-alkyl (45–65) (%)	O-alkyl (65–95) (%)	Di-O-alkyl and Some Aromatic (95–110) (%)	Aromatic (110–145) (%)	Phenolic (145–165) (%)	Carboxyl and Carbonyl (165–220) (%)	Alkyl/O-alkyl
Bulk soil Ag(Bh) (15–25 cm)[a]	37	13	26	6	12	3	3	0.82
Bulk O horizon leachate (DOC)[a]	28	11	24	6	13	5	13	0.67
Decaying coarse root	14	11	20	10	18	11	16	0.33
Organic accumulations at 20 cm	33	9	19	5	13	5	16	0.96
Organic accumulations at 60 cm	23	11	18	6	18	6	19	0.65

[a]M. G. Kramer (unpublished data). Alkyl to O-alkyl C ratios are calculated as the ratio of signal area from 0–45 ppm to 45–100 ppm.

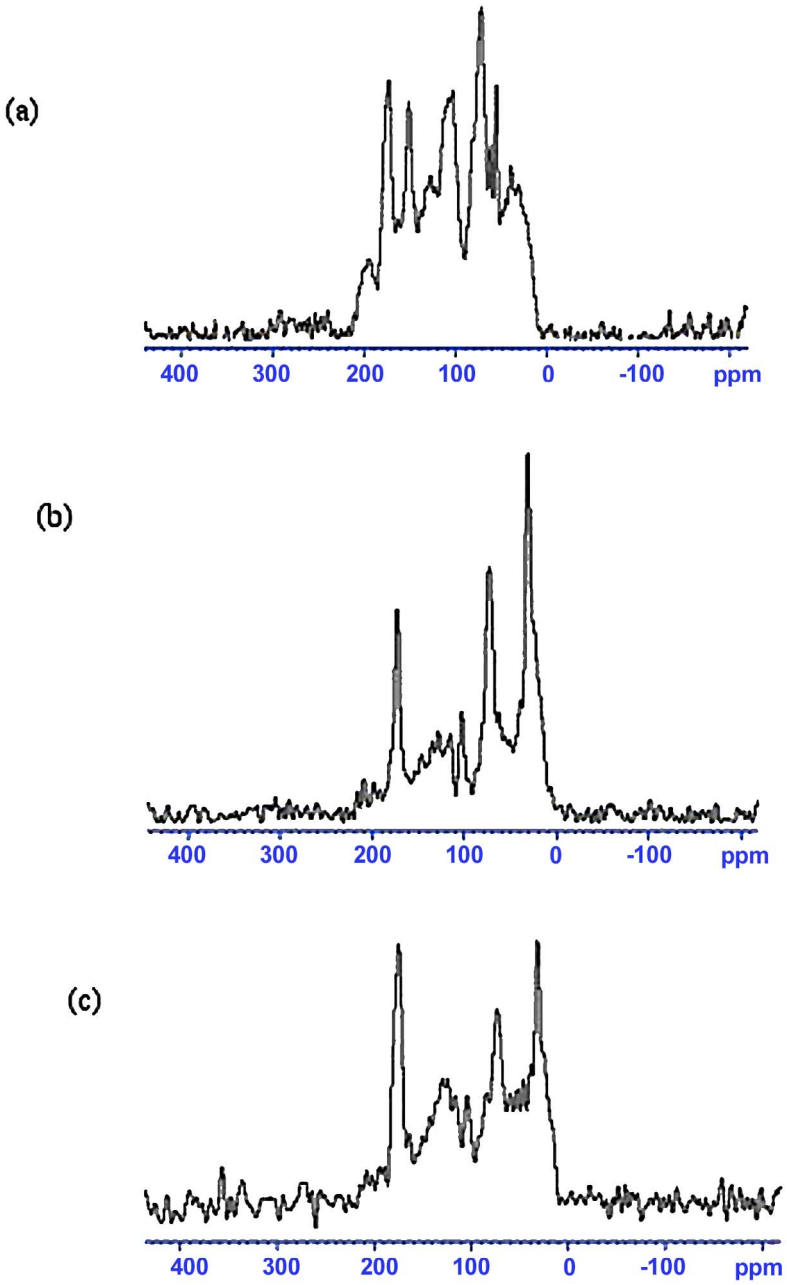

Figure 6. CP MAS ^{13}C-NMR spectra of (a) decaying roots from Bh and Bs and organic coatings on ped surfaces and infillings of macropore channels at (b) 20 cm depth and (c) 66 cm depth.

long-chain aliphatics (fatty acids, waxes and resins), either from the incorporation of microbial lipids or the selective preservation of plant lipids. This peak dominates the signal for organic thickenings at shallower depths in the soil profile (20 cm) but is less prominent in those deeper (60 cm), consistent with greater root-derived inputs at shallow depths. In contrast, the organic thickenings at 60 cm depth show stronger signal intensity in the aromatic C region as compared to the 20 cm sample, which may be indicative of oxidized lignin leached from fresh litter preferentially sorbed to SRO minerals at depth [*Kaiser and Guggenberger*, 2000; *Kalbitz and Kaiser*, 2008]. Another important feature in these OM coatings and infillings was the peak at 173 ppm, representing carboxyl groups in organic acids or amide groups in peptides [*Quideau et al.*, 2001]. Also present was a smaller peak at 130 ppm, which is indicative of aromatic structures, and may imply the presence of lignin phenols or char [*Skjemstad et al.*, 2002; *Hernes et al.*, 2007]. Ratios of alkyl-to-O-alkyl C increased in the order: decaying roots, organic coatings and infillings at 60 cm, and those at 20 cm, representing increased stage of decay (Table 2).

[24] Spectra for the surface mineral soil horizon (Ag (Bh)), where cracks and channels originate, were dominated by alkyl and O-alkyl C (Table 2). In contrast with organic

thickenings from the same depth, and for samples deeper in the soil profile, NMR spectra from near-surface mineral horizons had very low contributions of carboxyl and carbonyl C (Table 2). Leachate from the O horizon had a much higher contribution of carboxyl and carbonyl C, more similar to the organic infillings found at depth (Table 2). In fact, the relative distribution of different functional groups and alkyl-to-O-alkyl ratios for soil leachate and organic infillings found at 60 cm were remarkably similar, suggesting DOM might be a major source for the accumulation of C at depth.

3.4. Microbial Biomass C and N and Respiration Rates

[25] Extractable microbial biomass N (μg N g dry soil^{-1}) differed significantly between the three horizons sampled: Bh (10–18 cm depth) (45.3 ± 1.6), Bhsg (19–45 cm) (28.7 ± 2.1) and Bw (45–65 cm) (5.6 ± 1.3). Extractable microbial biomass C (μg C g dry soil^{-1}) differed significantly between the Bh (285.0 ± 27.0) and Bw (79.4 ± 8.6) horizons, with the Bhsg (167.0 ± 45.3) having intermediate values. However, all differences disappeared when biomass C and N were corrected for bulk-soil C and N concentrations for each horizon. Across all horizons, average extractable microbial biomass C and N were respectively: 3.6 ± 0.8 mg N g soil N^{-1} and 1.0 ± 0.3 mg C g soil C^{-1}. Microbial biomass C:N ratios were significantly higher in the Bw horizon (13.2 ± 2.2) than in the upper two mineral horizons, which together averaged 5.1 ± 0.5 (range: 3.1 to 6.6).

[26] Mean respiration rates normalized for soil C over the first 15 days of incubation were low for all samples, with statistically significant (ANOVA $F_{1,8} = 16.0197$, $r^2 = 0.84$, $p = 0.0039$) differences between all horizons: Bh (0.08 ± 0.002 mg C g soil C^{-1} day^{-1}), Bsg (0.07 ± 0.002 mg C g soil C^{-1} day^{-1}), and Bw (0.06 ± 0.004) mg C g soil C^{-1} day^{-1}).

3.5. Radiocarbon

[27] The Δ^{14}C content of bulk soil decreased with depth (Figure 7). Soil from the Oa horizon had Δ^{14}C values above zero, representing inputs of recent bomb-derived C (i.e., modern, fixed since the 1950–1960s). Deeper mineral horizons had conventional radiocarbon age (CRA) of over 1000 and 7000 years for the Bhsg and Bw/BS horizons, respectively (Table 3). The Δ^{14}C of organic C coatings and infillings also decreased (became older) with depth in the soil profile, but they were distinctly elevated above (younger, modern) the bulk mineral soil at the corresponding depth. Respired CO_2 from the laboratory incubations had much higher Δ^{14}C values (younger) than the bulk soil and the organic coatings in the same horizon, demonstrating that even in the deepest mineral horizons recent C was preferentially used by microorganisms (Figure 7). Notably, the DOC Δ^{14}C values were similar to values of bulk soils in the horizon above the lysimeter sampling point.

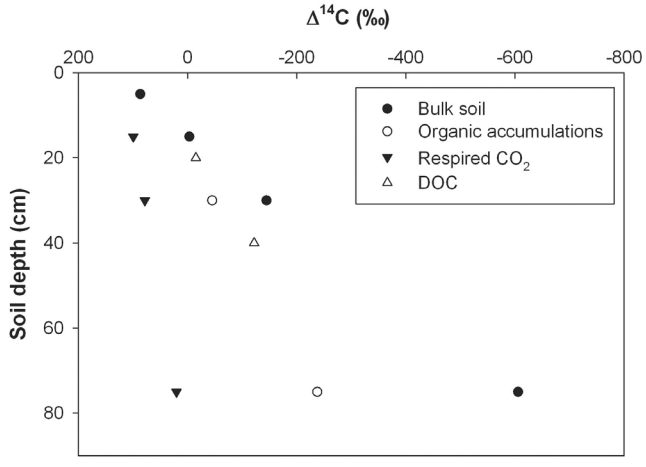

Figure 7. Radiocarbon concentrations for bulk soils, organic coatings on ped surfaces, and infillings of macropore channels, respired CO_2 from soil incubations, and DOC collected from lysimeters down the soil profile.

Table 3. Conventional Radiocarbon Ages of Bulk Horizons, Organic Accumulations, Respired CO_2 From Soil Lab Incubations, and DOC in Soil Water Collected From Zero-Tension Lysimeters in the Field[a]

	CRA (BP)
Bulk Horizons	
Oa	Modern
Bh[b]	Modern
Bhsg	1200 (20)
Bw/Bs[b]	7025 (28)
Organic Accumulations	
at 20 cm	315 (20)
at 66 cm	2120 (20)
Respired CO_2	
Bh	Modern
Bhsg	Modern
Bw/Bs	Modern
DOC	
Bh	65 (20)
Bg	98 (20)

[a]Standard errors are analytical errors on one field sample.
[b]Standard errors for these horizons are averages of two field sample replicates.

4. Discussion

4.1. Recent Surface Origin of OM Accumulating at Depth

[28] We synthesized morphological, spectroscopic, and isotopic data to determine the source and delivery mechanism for organic C in these SRO mineral rich soils. We find that minimally decomposed OM from surface organic horizons is being delivered to depth along nonreactive pathways, both in dissolved and particulate forms. Soil profiles exhibited thickenings and accumulations of very dark OM at 50–60 cm depth, representing significant deposition of organic C in deep mineral horizons. Bulk soils showed increasing C:N ratios with depth, suggesting accumulation of C-rich and N-poor OM that has not been thoroughly processed by microorganisms. The elevated C:N ratios of the deep mineral horizons matched those of fresh decomposing litter in the Oie and of DOM in soil solution. Extractable microbial biomass showed similar patterns in C:N ratios, paralleling depth differences in substrate stoichiometry.

[29] Wider soil C:N ratios in deeper horizons is relatively unusual and can be ascribed to processes that either deplete the store of N or protect OM from the normal biological decomposition processes that deplete C in organic substrate

relative to N. For instance in flooded soils, depleted O_2 leads to microbes switching to less efficient modes of metabolism and an accumulation of less decomposed OM [*Nadelhoffer and Fry*, 1988; *Bardy et al.*, 2008]. Higher C:N ratios at depth can also be attributed to a preferential loss of inorganic N or hydrolysis of components with high N content under strongly reducing conditions [*do Nascimento et al.*, 2004; *Bardy et al.*, 2008]. Our soils did show evidence of fluctuating redox conditions through mottling, high concentrations of dissolved total Fe in lysimeter solutions, and the deposition of oxidized Fe in the cemented horizon and along cracks between peds.

[30] However, fluctuating redox conditions cannot fully explain the depth-related C:N patterns at our site. In an earlier study, limited O_2 diffusivity was shown to slow down litter decomposition and lower N availability along a precipitation gradient on Maui, Hawai'i [*Schuur and Matson*, 2001]. While that study did not report soil C:N depth profiles to compare with our site, they did measure lower N availability and greatest soil C stocks at the sites with maximum annual precipitation (4000–5000 mm). However, this site also had the lowest SRO mineral content, as the soils were more highly weathered. Our site had lower rainfall and higher dominance of SRO minerals, so that the presence of reactive mineral surfaces appear to be more important in stabilizing soil C than reducing conditions [*Torn et al.*, 1997]. Furthermore, reducing conditions decrease with depth at our site, so that the deepest mineral horizons are more oxidized (redder) and contain fewer mottles than the overlying horizons. The observed pattern of enrichment in $\delta^{13}C$ with depth also follows what is expected from uncultivated, well-drained profiles [*Ehleringer et al.*, 2000; *Wynn et al.*, 2006], further suggesting that redox cannot explain the accumulation of OM with widening C:N ratios at depth.

[31] Further evidence from other studies on volcanic soils suggest that abundance of SRO minerals has a controlling effect on soil C:N trends, most likely through the stabilizing effect of highly reactive noncrystalline minerals on SOM. Similar patterns of increasing C:N ratio or maintenance of widening ratios with increasing soil depth have been reported for other Andisols dominated by SRO minerals under different climates and on substrates of varying age [*Conte et al.*, 2003; *Schrumpf et al.*, 2006; *Lilienfein et al.*, 2004; *Kawahigashi et al.*, 2003]. In contrast, nonallophanic soils show decreases in C:N with depth [*Conte et al.*, 2003; *Nierop et al.*, 2007], which is attributed to increased decomposition of plant-derived compounds and greater contributions of microbial bodies and products into SOM with depth in the absence of stabilizing SRO minerals [*Nadelhoffer and Fry*, 1988; *Baldock et al.*, 1992]. The preferential accumulation of hydrophobic OM with depth due to preferential removal from solution and adsorption to SRO mineral surfaces may also contribute to the widening of C:N ratios in deeper horizons [*Perakis and Hedin*, 2007].

[32] Spectral differences between OM collected from different depths are consistent with enrichment of material that has undergone less microbial processing in the deeper horizons. In particular, alkyl-to-O-alkyl ratios are expected to increase with soil depth, as OM typically becomes more decomposed, but the pattern we observe at Pu'u Eke is opposite, as was described with soil C:N ratios. The ratio of alkyl-to-O-alkyl C has been used extensively as an index of stage of microbial decay [*Baldock et al.*, 1997; *Kramer et al.*, 2003]. During plant litter decomposition and SOM formation, the dominant signal in the O-alkyl C region, from plant cellulose and hemicellulose, is progressively replaced by the alkyl C region. Alkyl C structures represent nonpolar, aliphatic compounds, such as waxes, resins and lipids; their accumulation in soils is attributed to selective preservation of recalcitrant plant compounds and/or to new production during microbial processing [*Kögel-Knabner et al.*, 1992; *Baldock et al.*, 1992; *Kögel-Knabner*, 2002; *Grandy and Neff*, 2008].

[33] Organic coatings and infillings at 20 cm had greater signal intensities in the alkyl C region than those from 60 cm, which had increasing contributions of aromatic C, carboxyl and carbonyl C. This is consistent with greater root inputs and microbial activity in surface horizons. The presence of a strong signal in the carboxyl-C regions of the spectra of macropore infillings and organic thickenings along ped surfaces suggest contributions from organic acids, likely a mix of microbial, plant and DOM inputs.

[34] Similar patterns of preferential accumulation of polysaccharides and carboxyl (acidic groups) and aromatic C with depth have been reported for other andic soils with SRO mineralogy [*Parfitt et al.*, 1999; *Conte et al.*, 2003; *Hiradate et al.*, 2006; *Bardy et al.*, 2008]. In contrast, nonandic soils typically show depletion of O-alkyl, carboxyl C and aromatic C and an enrichment in aliphatic C, representing a loss of carbohydrates and lignin with depth [*Conte et al.*, 2003; *Nierop et al.*, 2007]. In SRO mineral dominated soils, increased signal intensity in the aromatic region with depth is consistent with the preferential sorption of aromatic compounds in DOM, most likely derived from oxidized litter lignin, to highly reactive mineral surface, whose abundance increases with depth [*Torn et al.*, 1997; *Kaiser and Guggenberger*, 2000; *Kalbitz and Kaiser*, 2008].

[35] Examination of the soil profiles revealed the presence of extensive organic coatings along ped surfaces, similar to those reported in volcanic soils in Costa Rica [*Buurman et al.*, 2007] and other soils where illuviation of C is very high [*Bardy et al.*, 2008], in addition to black organic matter accumulations loosely infilling flow path channels. Our current methods do not allow us to identify biomarkers which would attribute the source of this OM to either above or belowground plant litter inputs or microbial inputs specifically (such as measuring cutin, suberin, amino sugars, or other microbial biomarkers [see *Otto and Simpson*, 2007]). However, morphological and chemical differences between brown decaying roots and black slimy coatings and channel infillings, and similarities between this OM accumulating at depth and DOC, suggest that in situ root decay is not the dominant mechanism for C deposition in the deepest mineral horizons at our sites. Live growing roots and decaying root channels certainly may have contributed to the development of a network of cracks and channels in the profile, and root exudates and decomposition products undoubtedly do contribute to DOC pools moving down the soil profile.

[36] Evidence that SOM in deep horizons is composed of a mixture of very young and old C is provided by the ^{14}C measurements. At the deepest horizon where $\Delta^{14}C$ was analyzed (50–60 cm), organic C in channel infillings and pockets had CRAs significantly younger (2000 years) than the bulk mineral horizon (7000 years). Modern $\Delta^{14}C$ values

of respired CO_2 from the short-term laboratory incubations indicate that microbes throughout the soil profile were accessing recent C, implying new C inputs occurring even at 60 cm depth. Modern radiocarbon ages of organic tongues, as deep as 60 and 100 cm in a matrix of bulk soil with CRA of several thousand years, were also reported by *Chabbi et al.* [2009].

4.2. Preferential Flow Paths Deliver MOC to Depth

[37] Carbon storage in these rain forest volcanic soils is linked to the movement of dissolved and particulate organic matter, which combined we refer to as mobile organic carbon (MOC), along infiltration pathways. Mineralogy and climate, in particular high interannual variability in rainfall [*Giambellucca et al.*, 1986], interact to create the right conditions for C to be delivered from the surface organic horizons to deep mineral horizons, where the potential for stabilization is greatest. SRO mineral rich soils are highly hydrated and shrink in response to periodic droughts such as El Niño events, which creates extensive cracks in subsurface B horizons. These cracks become pathways for the movement of MOC and metals during subsequent wet periods, both in dissolved and suspended form by gravitational flow.

[38] Open channels and cracks were very abundant at this site, and were infilled with loose, particulate OM and organic coatings, respectively. The presence of cracks and macropores were also reported for 22 soil pits in a highly weathered forest soil receiving 2500 mm mean annual precipitation in Hawai'i [*Lohse and Dietrich*, 2005]. Spectroscopic and chemical data of OM accumulating along the surfaces of cracks and in black pockets at depth matched material in the surface humic mineral horizons (Bh), where the network of cracks and channels are first observable. We therefore suggest that the explanation for high C:N ratios at depth is due primarily to recent origin of the organic material, rather than being a direct response to reducing conditions. Increasing soil C:N ratios with depth were also reported for Mediterranean basaltic soils where seasonal rainfall patterns lead to intense swelling and shrinking and visible deep surface cracking [*Barbera et al.*, 2008].

[39] Preferential flow paths can persist in soil profiles for decades to perhaps centuries and act as zones of C enrichment [*Hagedorn and Bundt*, 2002], as evidenced by high accumulations of organic matter with old radiocarbon ages found in the cracks and channels at our site. These pathways, while persistent, may also be very dynamic as they experience episodic, fast-moving flows during periods of high rainfall, which can explain very high rates of C accumulation compared to the bulk soil [*Hagedorn and Bundt*, 2002].

[40] High rainfall at the Pu'u Eke site (2800 to 3500 mm) during normal years ensures a constant supply of fresh DOM to the deeper horizons. The Oie, representing recent forest litter, is the zone of greatest production of DOC. DOC, Fe, and Al in solution decreased from the organic to the mineral horizons. Illuviation of DOM and metals is more commonly associated with podzolization than andic soil formation [*Ugolini et al.*, 1988; *Aran et al.*, 2001; *Ugolini and Dahlgren*, 2002], but clearly this process, through the formation of a network of cracks, contributes in a significant way to C sequestration and profile development in these soils. Preferential flow paths in the form of "tongues" have also recently been implicated in the delivery of modern C to deep horizons in an agricultural Mollisol (Cambisol) [*Chabbi et al.*, 2009]. Extensive organic "staining" of the soil profile has also been reported in a site with high rainfall (2450 mm MAP) characterized by very fast subsurface flow paths during intense rainstorms [*Graham et al.*, 2010].

4.3. Stabilization of Soil C at Depth

[41] The $\Delta^{14}C$ of both bulk soil and organic thickenings and channel infillings decreased significantly down the soil profile, representing stabilization of C pools, most likely due to interactions with Al in allophane and other SRO minerals [*Kleber et al.*, 2005; *Matus et al.*, 2006; *Egli et al.*, 2008]. The difference in age between surface and deep horizons was much greater for bulk soils than for the organic infillings, providing evidence for more dynamic transport of material in the preferential flow paths. Organic matter accumulating along ped surfaces and in macropore channels found at 60 cm, which show less microbial processing according to the NMR spectra and are more similar to DOM, had CRAs seven times greater than material at 20 cm with higher alkyl-to-O-alkyl ratios. The CRA of DOC collected under the Bh was only slightly older than the Oa and Bh horizons, which could be explained by heterogeneity in soil profiles. The CRA of bulk soil and DOC increased rapidly with depth. Old DOC has also been reported in an incubation study using enriched ^{13}C as a tracer [*Hagedorn et al.*, 2004]. Similar to what we saw, microbes in that study preferentially respired new, young C, leaving behind older C to contribute to the dissolved pool.

[42] Potential mechanisms contributing to C stabilization with depth include aging of C as it moves down the profile, interactions with mineral phases, and lower microbial activity in deeper horizons [*Fierer et al.*, 2003; *Holden and Fierer*, 2005; *Fontaine et al.*, 2007]. Stabilization of OM at depth in andic soils is most likely due to chemical interactions with Al in allophane and other SRO minerals [*Torn et al.*, 1997; *Kleber et al.*, 2005; *Egli et al.*, 2008]. At our site, MOC is likely stabilized from microbial decomposition as it moves down the soil profile by ligand sorption of Fe, and especially, Al [*Kalbitz et al.*, 2003; *Schwesig et al.*, 2003; *Scheel et al.*, 2007]. Material in the channels and OM pockets at our sites is enriched in Al relative to the bulk mineral horizons from the same depth. Lysimeter data show highest concentrations of Al and Fe under Oa horizons, potentially explained by enhanced mineral weathering at the Oa/Bh interface due to high concentrations of acidic organic compounds moving through solution.

[43] Both reduction processes and complexation with OM may serve to deliver Fe and Al along preferential flow paths and contribute to the formation of placic horizons, which are common in volcanic and spodic soils [*Farmer et al.*, 1983; *Jongmans et al.*, 2000; *Bardy et al.*, 2008]. At Pu'u Eke, the cemented, or placic, horizon is discontinuous and punctured by channels, which allows downward movement of C in dissolved as well as particulate forms. The highest mineral soil C:N ratio was measured in the placic Bhsm (43–47 cm) right below a Bg horizon, suggesting this OM originated in surface horizons and was delivered to deeper B horizons by dissolved flow along cracks.

[44] The presence of cemented or placic horizons may serve to separate zones of microbial activity, also contributing to the preservation of relatively undecomposed OM and the

old radiocarbon-based ages at depth. Ratios of Fe to Al show differences in redox chemistry above and below the cemented horizons, with upper horizons being depleted in Fe and enriched in Al, and lower horizons showing the opposite pattern. Soil morphology also exhibited evidence of reduction processes being more important above the placic, and oxidation dominating below.

[45] The stable N isotope data suggest similar trends in nitrogen dynamics. Enrichment in ^{15}N with depth, representing older, more decomposed material, and accompanied by a decrease in C:N ratios, is expected in undisturbed, well-drained profiles [*Ehleringer et al.*, 2000; *Hobbie and Ouimette*, 2009]. Stable C isotope data at our site show the expected enrichment with depth (even though C:N ratios do not), but ^{15}N data show the opposite pattern. Above the placic horizon, mineral soils are enriched in ^{15}N, while $\delta^{15}N$ of the soils below match that of the Oa1 horizon and approach $\delta^{15}N$ of atmospheric N inputs. Maximum $\delta^{15}N$ values in intermediate depths were observed in another Hawaiian wet tropical forest by *Schuur and Matson* [2001], a pattern common in high N soils dominated by arbuscular mycorrhizae [*Hobbie and Ouimette*, 2009]. Progressive depletion of ^{15}N below this intermediate maximum, which results in deeper soil profiles approaching isotopic composition of the organic horizons, could be due to illuviation of more recent OM or of ^{15}N depleted nitrate from the surface, or to fractionation during denitrification [*Hobbie and Ouimette*, 2009]. Further investigations on the form (organic versus inorganic) of N accumulating at depth and its $\delta^{15}N$ would help resolve this. Similar accumulations of OM depleted in ^{15}N and with CRAs several thousand years younger than the bulk soil, extending into deep mineral horizons in the forms of "organic tongues" have also been reported elsewhere [*Chabbi et al.*, 2009].

[46] Soil respiration rates at Pu'u Eke were much lower below the placic horizon, but radiocarbon data show that microbes are accessing recent inputs. Microbial community composition and distribution should be further explored, but at first approximation, extractable microbial biomass corrected by total soil C stocks did not differ between surface and deep mineral horizons.

[47] The stability of soil C at depth may help explain differences in oxidation above and below the placic horizons observed at our site. Soil C concentrations in deeper soils, while significantly less than in the surface horizons, remain high, but our data suggest that most of this C is potentially not bioavailable, so that microbes at depth are effectively experiencing an OM-free local environment. Respiration rates are very low and dominated by inputs of fresh C, suggesting microbes are not accessing the bulk SOM pool in deeper horizons. SOM accumulating at depth is enriched in aromatic acids, which have high capacity to bind to SRO minerals via carboxyl functional groups [*Kalbitz and Kaiser*, 2008; *Hernes et al.*, 2007]. These mineral-stabilized C pools can explain high MRTs measured at depth, as well as lower reduction below the placic horizon.

[48] Deep soil C storage at our site was significant: about 50% of total soil C stocks (375 ± 83 tC ha^{-1}) were located below 50 cm. These high soil C stocks are comparable to other tropical forest soils with similar rainfall on Andisols in Hawai'i [*Torn et al.*, 1997; *Schuur et al.*, 2001]. Soil C concentrations in the lowest depths remained very high (5–10%). The bulk soil C CRA increased significantly with depth: the Bh horizon at 10–12 cm depth was dominated by modern C, while below 60 cm, the CRA of soil C increased to almost 7000 years. Mean ages for bulk-soil C in the surface mineral horizon reflect fresh inputs of DOM and new litter in the form of POM. Increases in the CRA of bulk soil C with depth represents slowed decomposition with increasing mineral content [*Torn et al.*, 1997; *Fontaine et al.*, 2007].

5. Conclusions

[49] Morphological, chemical, and isotopic evidence show that the movement of OM in dissolved and particulate forms along infiltration pathways in soils is an important delivery mechanism for C and metals from organic horizons to deep mineral horizons. Hydrated SRO minerals are subject to strong shrinkage during occasional drought periods at annual-to-decadal time scales. The resulting structural cracks between peds in subsurface B horizons become pathways for DOM complexed with Fe and Al moving in soil solution during subsequent wet periods. Preferential flow of these organically rich solutes and/or colloids moves C to depth where C, Fe and Al are preferentially deposited on near-vertical crack surfaces and along near-horizontal flow surfaces at horizon boundaries. Long-term deposition forms discontinuous Fe- and OM-cemented lamella that serve to reinforce preferential flow paths. This transport mechanism for C and metal delivery to depth was accentuated in these sites given the conditions just discussed, but is likely an important pathway in all soils under different climates and mineralogy where biological activity, hydration, and weathering lead to the formation of channels and microfractures in soils and parent material.

[50] **Acknowledgments.** We would like to thank the following: for logistical support and access to field sites, Heraldo Farrington, Peter Vitousek, and Stuart Lau at Queen Emma Foundation, Parker Ranch, and for assistance with sample analyses, Katherine Lindeburg, Dasha Perkins, Frank Setaro, Rob Franks (UCSC Marine Analytical Lab), and Jerry Hu (UCSB Materials Research Lab). We thank Sean Schaeffer for help with microbial biomass data, Claudia Czimczik and Xiaomei Xu for radiocarbon analyses, and Ken Keefover-Ring for help with figures. We also would like to thank two anonymous reviewers for their thoughtful and helpful comments. This material is based upon work supported by the National Science Foundation under DEB grant 0610453 (to E.M.-S.) and USDA National Research Initiative grant 2007-35107-18429 (to M.G.K. and O.A.C.). M.S.C. was supported by the NOAA Climate and Global Change Postdoctoral Fellowship Program, administered by the University Corporation for Atmospheric Research.

References

Aran, D., M. Gury, and E. Jeanroy (2001), Organo-metallic complexes in an andosol: A comparative study with a cambisol and podzol, *Geoderma*, *99*, 65–79, doi:10.1016/S0016-7061(00)00064-1.

Baisden, W. T., R. Amundson, D. L. Brenner, A. C. Cook, C. Kendall, and J. W. Harden (2002), A multiisotope C and N modeling analysis of soil organic matter turnover and transport as a function of soil depth in a California annual grassland soil chronosequence, *Global Biogeochem. Cycles*, *16*(4), 1135, doi:10.1029/2001GB001823.

Baker, J. M., T. W. Ochsner, R. T. Venterea, and T. J. Griffis (2007), Tillage and soil carbon sequestration—What do we really know?, *Agric. Ecosyst. Environ.*, *118*, 1–5, doi:10.1016/j.agee.2006.05.014.

Baldock, J. A., J. M. Oades, A. G. Waters, X. Peng, A. M. Vassallo, and M. A. Wilson (1992), Aspects of the chemical structure of soil organic materials as revealed by solid-state ^{13}C NMR spectroscopy, *Biogeochemistry*, *16*, 1–42.

Baldock, J. A., J. M. Oades, P. N. Nelson, T. M. Skene, A. Golchin, and P. Clarke (1997), Assessing the extent of decomposition of natural

organic materials using solid-state ^{13}C NMR spectroscopy, *Aust. J. Soil Res.*, *35*, 1061–1083, doi:10.1071/S97004.

Baldock, J. A., C. A. Masiello, Y. Gelinas, and J. I. Hedges (2004), Cycling and composition of organic matter in terrestrial and marine ecosystems, *Mar. Chem.*, *92*, 39–64, doi:10.1016/j.marchem.2004.06.016.

Barbera, V., S. Raimondi, M. Egli, and M. Plötze (2008), The influence of weathering processes on labile and stable organic matter in Mediterranean volcanic soils, *Geoderma*, *143*, 191–205, doi:10.1016/j.geoderma.2007.11.002.

Bardy, M., E. Fritsch, S. Derenne, T. Allard, N. R. do Nascimento, and G. T. Bueno (2008), Micromorphology and spectroscopic characteristics of organic matter in waterlogged podzols of the upper Amazon basin, *Geoderma*, *145*, 222–230, doi:10.1016/j.geoderma.2008.03.008.

Bascomb, C. L. (1968), Distribution of pyrophosphate-extractable iron and organic carbon in soils of various groups, *J. Soil Sci.*, *19*, 251–268, doi:10.1111/j.1365-2389.1968.tb01538.x.

Batjes, N. H., and W. G. Sombroek (1997), Possibilities for carbon sequestration in tropical and subtropical soils, *Global Change Biol.*, *3*, 161–173, doi:10.1046/j.1365-2486.1997.00062.x.

Blake, G. R., and K. H. Hartge (1986), Bulk density, in *Methods of Soil Analysis, Part 1. Physical and Mineralogical Methods*, edited by A. Klute, pp. 363–376, Am. Soc. of Agron., Madison, Wis.

Buurman, P., F. Peterse, and G. Almendros Martin (2007), Soil organic matter chemistry in allophanic soils: A pyrolysis-GC/MS study of a Costa Rican andosol catena, *Eur. J. Soil Sci.*, *58*, 1330–1347, doi:10.1111/j.1365-2389.2007.00925.x.

Cabrera, M. L., and M. H. Beare (1993), Alkaline persulfate oxidation for determining total nitrogen in microbial biomass extracts, *Soil Sci. Soc. Am. J.*, *57*, 1007–1012, doi:10.2136/sssaj1993.03615995005700040021x.

Chabbi, A., I. Kogel-Knabner, and C. Rumpel (2009), Stabilised carbon in subsoil horizons is located in spatially distinct parts of the soil profile, *Soil Biol. Biochem.*, *41*, 256–261, doi:10.1016/j.soilbio.2008.10.033.

Chadwick, O. A., R. T. Gavenda, E. F. Kelly, K. Ziegler, C. G. Olson, W. C. Elliott, and D. M. Hendricks (2003), The impact of climate on the biogeochemical functioning of volcanic soils, *Chem. Geol.*, *202*, 195–223, doi:10.1016/j.chemgeo.2002.09.001.

Chorover, J., M. K. Amistadi, and O. A. Chadwick (2004), Surface charge evolution of mineral-organic complexes during pedogenesis in Hawaiian basalt, *Geochim. Cosmochim. Acta*, *68*, 4859–4876, doi:10.1016/j.gca.2004.06.005.

Conte, P., R. Spaccini, M. Chiarella, and A. Piccolo (2003), Chemical properties of humic substances in soils of an Italian volcanic system, *Geoderma*, *117*, 243–250, doi:10.1016/S0016-7061(03)00126-5.

do Nascimento, N. R., G. T. Bueno, E. Fritsch, A. J. Herbillon, T. Allard, A. J. Melfi, R. Astolfo, H. Boucher, and Y. Li (2004), Podzolization as a deferralitization process: A study of an acrisol-podzol sequence derived from Paleozoic sandstones in the northern upper Amazon Basin, *Eur. J. Soil Sci.*, *55*, 523–538, doi:10.1111/j.1365-2389.2004.00616.x.

Doyle, A., M. N. Weintraub, and J. P. Schimel (2004), Persulfate digestion and simultaneous colorimetric analysis of carbon and nitrogen in soil extracts, *Soil Sci. Soc. Am. J.*, *68*, 669–676, doi:10.2136/sssaj2004.0669.

Egli, M., M. Nater, A. Mirabella, S. Raimondi, M. Plötze, and L. Alioth (2008), Clay minerals, oxyhydroxide formation, element leaching and humus development in volcanic soils, *Geoderma*, *143*, 101–114, doi:10.1016/j.geoderma.2007.10.020.

Ehleringer, J. R., N. Buchmann, and L. B. Flanagan (2000), Carbon isotope ratios in belowground carbon cycle processes, *Ecol. Appl.*, *10*, 412–422, doi:10.1890/1051-0761(2000)010[0412:CIRIBC]2.0.CO;2.

Ellerbrock, R. H., H. H. Gerke, and C. Böhm (2009), In situ DRIFT characterization of organic matter composition on soil structural surfaces, *Soil Sci. Soc. Am. J.*, *73*, 531–540, doi:10.2136/sssaj2008.0103.

Farmer, V. C., J. O. Skjemstad, and C. H. Thompson (1983), Genesis of humus B horizons in hydromorphic humus podzols, *Nature*, *304*, 342–344, doi:10.1038/304342a0.

Fierer, N., and J. P. Schimel (2003), A proposed mechanism for the pulse in carbon dioxide production commonly observed following the rapid rewetting of a dry soil, *Soil Sci. Soc. Am. J.*, *67*, 798–805, doi:10.2136/sssaj2003.0798.

Fierer, N., J. Schimel, and P. Holden (2003), Variations in microbial community composition through two soil depth profiles, *Soil Biol. Biochem.*, *35*, 167–176, doi:10.1016/S0038-0717(02)00251-1.

Fontaine, S., S. Barot, P. Barré, N. Bdioui, B. Mary, and C. Rumpel (2007), Stability of organic carbon in deep soil layers controlled by fresh carbon supply, *Nature*, *450*, 277–280, doi:10.1038/nature06275.

Giambellucca, T. W., M. A. Nullet, and T. A. Schroeder (1986), *Rainfall Atlas of Hawaii*, Dep. of Land and Nat. Resour., Honolulu, Hawaii.

Graham, C. B., R. A. Woods, and J. J. McDonnell (2010), Hillslope threshold response to rainfall: (1) A field based forensic approach, *J Hydrol.*, *393*, 65–76, doi:10.1016/j.jhydrol.2009.12.015.

Grandy, A. S., and J. C. Neff (2008), Molecular C dynamics downstream: The biochemical decomposition sequence and its impact on soil organic matter structure and function, *Sci. Total Environ.*, *404*, 297–307, doi:10.1016/j.scitotenv.2007.11.013.

Hagedorn, F., and M. Bundt (2002), The age of preferential flow paths, *Geoderma*, *108*, 119–132, doi:10.1016/S0016-7061(02)00129-5.

Hagedorn, F., M. Saurer, and P. Blaser (2004), A ^{13}C tracer study to identify the origin of dissolved organic carbon in forested mineral soils, *Eur. J. Soil Sci.*, *55*, 91–100, doi:10.1046/j.1365-2389.2003.00578.x.

Hernes, P. J., A. C. Robinson, and A. K. Aufdenkampe (2007), Fractionation of lignin during leaching and sorption and implications for organic matter "freshness," *Geophys. Res. Lett.*, *34*, L17401, doi:10.1029/2007GL031017.

Hiradate, S., H. Hirai, and H. Hashimoto (2006), Characterization of allophanic andisols by solid-state ^{13}C, ^{27}Al, and ^{29}Si NMR and by C stable isotope ratio, $\delta^{13}C$, *Geoderma*, *136*, 696–707, doi:10.1016/j.geoderma.2006.05.007.

Hobbie, E. A., and A. P. Ouimette (2009), Controls on nitrogen isotope patterns in soil profiles, *Biogeochemistry*, *95*, 355–371, doi:10.1007/s10533-009-9328-6.

Holden, P. A., and N. Fierer (2005), Microbial processes in the vadose zone, *Vadose Zone J.*, *4*, 1–21.

Hotchkiss, S., P. M. Vitousek, O. A. Chadwick, and J. Price (2000), Climate cycles, geomorphological change, and the interpretation of soil and ecosystem development, *Ecosystems*, *3*, 522–533, doi:10.1007/s100210000046.

Jobbágy, E., and R. B. Jackson (2000), The vertical distribution of soil organic carbon and its relation to climate and vegetation, *Ecol. Appl.*, *10*, 423–436, doi:10.1890/1051-0761(2000)010[0423:TVDOSO]2.0.CO;2.

Jongmans, A. G., L. Denaix, F. van Oort, and A. Nieuwenhuyse (2000), Induration of C horizons by allophane and imogolite in Costa Rican volcanic soils, *Soil Sci. Soc. Am. J.*, *64*, 254–262, doi:10.2136/sssaj2000.641254x.

Kaiser, K., and G. Guggenberger (2000), The role of DOM sorption to mineral surfaces in the preservation of organic matter in soils, *Org. Geochem.*, *31*, 711–725.

Kalbitz, K., and K. Kaiser (2008), Contribution of dissolved organic matter to carbon storage in forest mineral soils, *J. Plant Nutr. Soil Sci.*, *171*, 52–60.

Kalbitz, K., D. Schwesig, J. Schmerwitz, K. Kaiser, L. Haumaier, B. Glaser, R. Ellerbock, and P. Leinweber (2003), Changes in properties of soil-derived dissolved organic matter induced by biodegradation, *Soil Biol. Biochem.*, *35*, 1129–1142, doi:10.1016/S0038-0717(03)00165-2.

Kawahigashi, M., H. Sumida, and K. Yamamoto (2003), Seasonal changes in organic compounds in soil solutions obtained from volcanic ash soils under different land uses, *Geoderma*, *113*, 381–396, doi:10.1016/S0016-7061(02)00371-3.

Kleber, M., R. Mikutta, M. S. Torn, and R. Jahn (2005), Poorly crystalline mineral phases protect organic matter in acid subsoil horizons, *Eur. J. Soil Sci.*, *56*, 717–725.

Kögel-Knabner, I. (1997), ^{13}C and ^{15}N NMR spectroscopy as a tool in soil organic matter studies, *Geoderma*, *80*, 243–270, doi:10.1016/S0016-7061(97)00055-4.

Kögel-Knabner, I. (2000), Analytical approaches for characterizing soil organic matter, *Org. Geochem.*, *31*, 609–625, doi:10.1016/S0146-6380(00)00042-5.

Kögel-Knabner, I. (2002), The macromolecular organic composition of plant and microbial residues as inputs to soil organic matter, *Soil Biol. Biochem.*, *34*, 139–162, doi:10.1016/S0038-0717(01)00158-4.

Kögel-Knabner, I., J. W. de Leeuw, and P. G. Hatcher (1992), Nature and distribution of alkyl carbon in forest soil profiles: Implications for the origin and humification of aliphatic biomacromolecules, *Sci. Total Environ.*, *117–118*, 175–185, doi:10.1016/0048-9697(92)90085-7.

Kramer, M. G., P. Sollins, R. S. Sletten, and P. K. Swart (2003), N isotope fractionation and measures of organic matter alteration during decomposition, *Ecology*, *84*, 2021–2025.

Leue, M., R. H. Ellerbrock, and H. H. Gerke (2010), DRIFT mapping of organic matter composition at intact soil aggregate surfaces, *Vadose Zone J.*, *9*, 317–324, doi:10.2136/vzj2009.0101.

Lilienfein, J., R. G. Qualls, S. M. Uselman, and S. D. Bridgham (2004), Adsorption of dissolved organic carbon and nitrogen in soils of a weathering chronosequence, *Soil Sci. Soc. Am. J.*, *68*, 292–305, doi:10.2136/sssaj2004.2920.

Lohse, K. A., and W. E. Dietrich (2005), Contrasting effects of soil development on hydrological properties and flow paths, *Water Resour. Res.*, *41*, W12419, doi:10.1029/2004WR003403.

Lorenz, K., and R. Lal (2005), The depth distribution of soil organic carbon in relation to land use and management and the potential of carbon sequestration in subsoil horizons, *Adv. Agron.*, *88*, 35–66, doi:10.1016/S0065-2113(05)88002-2.

Matus, F., X. Amigo, and S. M. Kristiansen (2006), Aluminium stabilization controls organic carbon levels in Chilean volcanic soils, *Geoderma*, *132*, 158–168, doi:10.1016/j.geoderma.2005.05.005.

McKeague, J. A., and J. H. Day (1966), Dithionite- and oxalate extractable Fe and Al as aids in differentiating various classes of soils, *Can. J. Soil Sci.*, *46*, 13–22, doi:10.4141/cjss66-003.

Mehra, O. P., and M. L. Jackson (1958), Iron oxide removal from soils and clays by a dithionite-citrate system buffered with sodium bicarbonate, *Clays Clay Miner.*, *7*, 317–327, doi:10.1346/CCMN.1958.0070122.

Michalzik, B., E. Tipping, J. Mulder, J. F. Gallardo Lancho, E. Matzner, C. L. Bryant, N. Clarke, S. Lofts, and M. A. Vicente Esteban (2003), Modelling the production and transport of dissolved organic carbon in forest soils, *Biogeochemistry*, *66*, 241–264, doi:10.1023/B:BIOG.0000005329.68861.27.

Nadelhoffer, K. J., and B. Fry (1988), Controls on natural nitrogen-15 and carbon-13 abundances in forest soil organic matter, *Soil Sci. Soc. Am. J.*, *52*, 1633–1640, doi:10.2136/sssaj1988.03615995005200060024x.

Nepstad, D. C., C. R. De Carvalho, E. A. Davidson, P. H. Jipp, P. A. Lefebvre, G. H. Negreiros, E. D. Da Silva, T. A. Stone, S. E. Trumbore, and S. Vieira (1994), The role of deep roots in the hydrological and carbon cycle of Amazonian forests and pastures, *Nature*, *372*, 666–669.

Nierop, K. G. J., F. H. Tonneijck, B. Jansen, and J. M. Verstraten (2007), Organic matter in volcanic ash soils under forest and páramo along an Ecuadorian altitudinal transect, *Soil Sci. Soc. Am. J.*, *71*, 1119–1127, doi:10.2136/sssaj2006.0322.

Otto, A., and M. J. Simpson (2007), Analysis of soil organic matter biomarkers by sequential chemical degradation and gas chromatography–mass spectrometry, *J. Sep. Sci.*, *30*, 272–282, doi:10.1002/jssc.200600243.

Parfitt, R. L., G. Yuan, and B. K. G. Theng (1999), A ^{13}C-NMR study of the interactions of soil organic matter with aluminium and allophane in podzols, *Eur. J. Soil Sci.*, *50*, 695–700, doi:10.1046/j.1365-2389.1999.00274.x.

Perakis, S. S., and L. O. Hedin (2007), State factor relationships of dissolved organic carbon and nitrogen losses from unpolluted temperate forest watersheds, *J. Geophys. Res.*, *112*, G02010, doi:10.1029/2006JG000276.

Porder, S., and O. A. Chadwick (2009), Climate and soil-age constraints on nutrient uplift and retention by plants, *Ecology*, *90*, 623–636, doi:10.1890/07-1739.1.

Porder, S., G. E. Hilley, and O. A. Chadwick (2007), Chemical weathering, mass loss, and dust inputs across a climate by time matrix in the Hawaiian islands, *Earth Planet. Sci. Lett.*, *258*, 414–427, doi:10.1016/j.epsl.2007.03.047.

Preston, C. M. (2001), Carbon-13 solid-state NMR of soil organic matter—Using the technique effectively, *Can. J. Soil Sci.*, *81*, 255–270.

Quideau, S. A., M. A. Anderson, R. C. Graham, O. A. Chadwick, and S. E. Trumbore (2001), A direct link between forest vegetation type and soil organic matter composition, *Geoderma*, *104*, 41–60, doi:10.1016/S0016-7061(01)00055-6.

Richter, D., Jr., and D. Markewitz (1995), How deep is soil?, *BioScience*, *45*, 600–609, doi:10.2307/1312764.

Richter, D., Jr., and M. L. Mobley (2009), Monitoring Earth's critical zone, *Science*, *326*, 1067–1068, doi:10.1126/science.1179117.

Rumpel, C., K. Eusterhues, and I. Kögel-Knabner (2004), Location and chemical composition of stabilized organic carbon in topsoil and subsoil horizons of two acid forest soils, *Soil Biol. Biochem.*, *36*, 177–190, doi:10.1016/j.soilbio.2003.09.005.

Scheel, T., C. Dörfler, and K. Kalbitz (2007), Precipitation of dissolved organic matter by aluminum stabilizes carbon in acidic forest soils, *Soil Sci. Soc. Am. J.*, *71*, 64–74.

Schrumpf, M., W. Zech, J. Lehmann, and H. V. C. Lyaruu (2006), TOC, TON, TOS and TOP in rainfall, throughfall, litter percolate and soil solution of a montane rain forest succession at Mt. Kilimanjaro, Tanzania, *Biogeochemistry*, *78*, 361–387, doi:10.1007/s10533-005-4428-4.

Schuur, E. A. G., and P. A. Matson (2001), Net primary productivity and nutrient cycling across a mesic to wet precipitation gradient in Hawaiian montane forest, *Oecologia*, *128*, 431–442.

Schuur, E. A. G., and S. E. Trumbore (2006), Partitioning sources of soil respiration in boreal black spruce forest using radiocarbon, *Global Change Biol.*, *12*, 165–176, doi:10.1111/j.1365-2486.2005.01066.x.

Schuur, E. A. G., O. A. Chadwick, and P. A. Matson (2001), Carbon cycling and soil carbon storage in mesic to wet Hawaiian montane forests, *Ecology*, *82*, 3182–3196, doi:10.1890/0012-9658(2001)082[3182:CCASCS]2.0.CO;2.

Schwendenmann, L., and E. Veldkamp (2005), The role of dissolved organic carbon, dissolved organic nitrogen, and dissolved inorganic nitrogen in a tropical wet forest ecosystem, *Ecosystems*, *8*, 339–351, doi:10.1007/s10021-003-0088-1.

Schwesig, D., K. Kalbitz, and E. Matzner (2003), Effects of aluminium on the mineralization of dissolved organic carbon derived from forest soils, *Eur. J. Soil Sci.*, *54*, 311–322, doi:10.1046/j.1365-2389.2003.00523.x.

Skjemstad, J. O., D. C. Reicosky, A. R. Wilts, and J. A. McGowan (2002), Charcoal carbon in U.S. agricultural soils, *Soil Sci. Soc. Am. J.*, *66*, 1249–1255, doi:10.2136/sssaj2002.1249.

Soil Survey Laboratory Staff (1992), *Soil Survey Laboratory Methods Manual, Version 2.0*, *Soil Surv. Invest. Rep. 42*, U.S. Dep. of Agric., Washington, D. C.

Soil Survey Staff (1999), *Soil Taxonomy: A Basic System of Soil Classification for Making and Interpreting Soil Surveys*, 2nd ed., U.S. Dep. of Agric. Soil Conserv. Serv., Washington, D. C.

Southon, J., G. Santos, K. Druffel-Rodriguez, E. Druffel, S. Trumbore, X. Xu, S. Griffin, S. Ali, and M. Mazon (2004), The Keck Carbon Cycle AMS Laboratory, University of California, Irvine: Initial operation and a background surprise, *Radiocarbon*, *46*, 41–49.

Spengler, S. R., and M. O. Garcia (1988), Geochemistry of the Hawi lavas, Kohala Volcano, Hawaii, *Contrib. Mineral. Petrol.*, *99*, 90–104, doi:10.1007/BF00399369.

Stuiver, M., and H. A. Polach (1977), Reporting of ^{14}C data, *Radiocarbon*, *19*, 355–363.

Torn, M., S. Trumbore, O. Chadwick, P. Vitousek, and D. Hendricks (1997), Mineral control of soil organic carbon storage and turnover, *Nature*, *389*, 170–173, doi:10.1038/38260.

Trumbore, S. (2000), Age of soil organic matter and soil respiration: Radiocarbon constraints on belowground C dynamics, *Ecol. Appl.*, *10*, 399–411, doi:10.1890/1051-0761(2000)010[0399:AOSOMA]2.0.CO;2.

Trumbore, S. (2009), Radiocarbon and soil carbon dynamics, *Annu. Rev. Earth Planet. Sci.*, *37*, 47–66, doi:10.1146/annurev.earth.36.031207.124300.

Ugolini, F. C., and R. Dahlgren (2002), Soil development in volcanic ash, *Global Environ. Res.*, *6*, 69–81.

Ugolini, F. C., R. Dahlgren, S. Shoji, and T. Ito (1988), An example of andosolization and podzolization as revealed by soil solution studies, southern Hakkoda, northeastern Japan, *Soil Sci.*, *145*, 111–125, doi:10.1097/00010694-198802000-00005.

Veldkamp, E., A. Becker, L. Schwendemann, D. A. Clark, and H. Schulte-Bisping (2003), Substantial labile carbon stocks and microbial activity in deeply weathered soils below a tropical wet forest, *Global Change Biol.*, *9*, 1171–1184, doi:10.1046/j.1365-2486.2003.00656.x.

Wada, K. (1989), Allophane and imogolite, in *Minerals in Soil Environments*, 2nd ed., edited by J. B. Dixon and S. B. Weed, pp. 1051–1087, Soil Sci. Soc. of Am., Madison, Wis.

Wolfe, E. W., and J. Morris (1996), Geologic map of the Island of Hawaii, *Map I-2524A*, U.S. Geol. Surv., Denver, Colo.

Wynn, J. G., J. W. Harden, and T. L. Fries (2006), Stable carbon isotope depth profiles and soil organic carbon dynamics in the lower Mississippi Basin, *Geoderma*, *131*, 89–109, doi:10.1016/j.geoderma.2005.03.005.

Xu, X., S. E. Trumbore, S. Zheng, J. R. Southon, K. E. McDuffee, M. Luttgen, and J. C. Liu (2007), Modifying a sealed tube zinc reduction method for preparation of AMS graphite targets: Reducing background and attaining high precision, *Nucl. Instrum. Methods Phys. Res., Sect. B*, *259*, 320–329, doi:10.1016/j.nimb.2007.01.175.

M. S. Carbone and O. A. Chadwick, Department of Geography, University of California, Santa Barbara, CA 93106-4060, USA.

M. Kramer, Earth and Planetary Sciences Department, University of California, Santa Cruz, CA 95064, USA.

E. Marin-Spiotta, Department of Geography, University of Wisconsin-Madison, Madison, WI 53706, USA. (marinspiotta@wisc.edu)